

Adaptive Tracking Control of On-Line Path Planners: Velocity Fields and Navigation Functions*

M. L. McIntyre,[†] W. E. Dixon,[‡] D. M. Dawson,[†] and B. Xian[†]

[†]Department of Electrical & Computer Engineering, Clemson University, Clemson, SC 29634-0915

[‡]Eng. Science and Tech. Div. - Robotics, Oak Ridge Nat. Laboratory, P.O. Box 2008, Oak Ridge, TN 37831-6305

E-mail: dixonwe@ornl.gov

Abstract: Traditionally, robot control research has focused on the position tracking problem where the objective is to force the robot to follow an a priori known desired time dependent trajectory. Motivated by task objectives that are more effectively described by on-line, state-dependent trajectories, two adaptive tracking controllers are developed in this paper that accommodate on-line path planning objectives. An example adaptive controller is first modified to achieve velocity field tracking in the presence of parametric uncertainty in the robot dynamics. The development aims to relax the typical assumption that the integral of the velocity field is bounded by incorporating a norm squared gradient term the control design so that the boundedness of all signals can be proven. An extension is then provided that targets the trajectory planning problem where the task objective can be described as the desire to move to a goal configuration while avoiding known obstacles. Specifically, an adaptive navigation function based controller is designed to provide a path from an initial condition inside the free configuration space of the robot manipulator to the goal configuration. Simulation for each controller are provided to illustrate the performance of the approaches.

1 Introduction

Traditionally, robot control researchers have focused on the position tracking problem where the objective is to force the robot to follow a desired time dependent trajectory. Since the objective is encoded in terms of a time dependent trajectory, the robot may be forced to follow an unknown course to catch up with the desired trajectory in the presence of a large initial error. For example, several researchers (e.g., [5], [30]) have reported the so called radial reduction phenomena in which the actual path followed has a smaller radius than the specified trajectory. In light of this phenomena, the control objective for many robotic tasks are more appropriately encoded as a contour following problem in which the objective is to force the robot to follow a state-dependent function that describes the contour. One example of a control strategy aimed at the contour following problem is velocity field control (VFC) where the desired contour is describe by a velocity tangent vector

*This research was supported in part U.S. DOE Office of Biological and Environmental Research (OBER) Environmental Management Sciences Program (EMSP) project ID No. 82797 at ORNL, and by U.S. NSF Grant DMI-9457967, ONR Grant N00014-99-1-0589, a DOC Grant, an ARO Automotive Center Grant, and in part by the Defence Advanced Research Project Agency (DARPA) through the Space Naval Warfare System Center, San Diego, contract N66001-03-R-8043.

[21]. The advantages of the VFC approach can be summarized as follows.¹

- The velocity field error more effectively penalizes the robot for leaving the desired contour.
- The control task can be specified invariant of the task execution speed.
- Task coordination and synchronization is more explicit for contour following.

The ability for a velocity field to encode certain contour following tasks has recently prompted researchers to investigate VFC for various applications. For example, Li and Horowitz utilized a passive VFC approach to control robot manipulators for contour following applications in [21], and more recently, Dee and Li used VFC to achieve passive bilateral teleoperation of robot manipulators in [29]. The authors of [30] utilized a passive VFC approach to develop a force controller for robot manipulator contour following applications. Yamakita et al. investigated the application of passive VFC to cooperative mobile robots and cooperative robot manipulators in [33] and [34], respectively. Typically, VFC is based on a nonlinear control approach where exact model knowledge of the system dynamics are required. Motivated by the desire to account for uncertainty in the robot dynamics, Cervantes et al. developed a robust VFC in [5]. Specifically, in [5] a proportional-integral controller was developed that achieved semiglobal practical stabilization of the velocity field tracking errors despite uncertainty in the robot dynamics. From a review of VFC literature, it can also be determined that previous research efforts have focused on ensuring the robot tracks the velocity field, but no development has been provided to ensure the joint angle remains bounded. The result in [5] acknowledged the issue of boundedness of the robot position; however, the issue is simply addressed by an assumption that the following norm

$$\left\| q(0) + \int_0^t \vartheta(q(\sigma)) d\sigma \right\| \quad (1)$$

yields globally bounded trajectories, where $q(t)$ denotes the position, and $\vartheta(\cdot)$ denotes the velocity field.

In addition to VFC, some task objectives are motivated by the need follow a trajectory to a desired goal configuration while avoiding known obstacles in the configuration space. For this class of problems, it is more important for the robot to follow an obstacle free path to the desired goal point than it is to meet a time-based requirement. Numerous researchers have investigated algorithms to address this motion control problem. A comprehensive summary of techniques that address the classic geometric problem of constructing a collision-free path and traditional path planning algorithms is provided in Section 9, “Literature Landmarks”, of Chapter 1 of [20]. Since the pioneering work by Khatib in [14], it is clear that the construction and use of potential functions has continued to be one of the mainstream approaches to robotic task execution among known obstacles. In short, potential functions produce a repulsive potential field around the robot workspace boundary and obstacles and an attractive potential field at the goal configuration. A comprehensive overview of research directed at potential functions is provided in [20]. One of criticisms of the potential function approach is that local minima can occur that can cause the robot to “get stuck” without reaching the goal position. Several researchers have proposed approaches to address the local minima issue (e.g., see [3], [4], [6], [15], [27]). One approach to address the local minima issue was provided by Koditschek in [17] for holonomic systems (see also [18] and [23]) that is based on a

¹See [5], [21], and [30] for a more thorough discussion of the advantages and differences of VFC with respect to traditional trajectory tracking control.

special kind of potential function, coined a navigation function, that has a refined mathematical structure which guarantees a unique minimum exists. By leveraging from previous results directed at classic (holonomic) systems, more recent research has focused on the development of potential function-based approaches for nonholonomic systems. For a review of this literature see [2], [10], [11], [12], [16], [19], [22], [23], [25], and [26].

The aim of this paper is to illustrate how an example adaptive controller (e.g., the benchmark adaptive tracking controller presented in [24]) can be modified to incorporate trajectory planning techniques with the controller. To this end, two adaptive controllers are developed. The first controller focuses on the VFC problem. Specifically, the benchmark adaptive controller given in [24] is modified to yield VFC in the presence of parametric uncertainty. The contribution of the development is that velocity field tracking is achieved by incorporating a norm squared gradient term in the control design that is used to prove the joint angles are bounded through a Lyapunov-analysis rather than by an assumption. In lieu of the assumption in (1), the VFC development is based on the assumption that the velocity field is first order differentiable, and that a first order differentiable, nonnegative function $V(q) \in \mathbb{R}$ exists such that the following inequality holds

$$\frac{\partial V(q)}{\partial q} \vartheta(q) \leq -\gamma_3(q) + \zeta_0 \quad (2)$$

where $\frac{\partial V(q)}{\partial q}$ denotes the partial derivative of $V(q)$ with respect to $q(t)$, $\gamma_3(\cdot) \in \mathbb{R}$ is a class \mathcal{K} function², and $\zeta_0 \in \mathbb{R}$ is a nonnegative constant. It is interesting to note that the Mean Value Theorem can be applied to the velocity field described in the experimental results provided in [5] to illustrate the validity of (2). As an extension to the VFC problem, a navigation function is incorporated with the benchmark adaptive controller in [24] (by also injecting a gradient term) to track a reference trajectory that yields a collision free path to a constant goal point in an obstacle cluttered environment with known obstacles.

This paper is organized as follows. In Section 2, the dynamic model for a robot manipulator is provided. In Section 3, the VFC development is presented, including a two-part stability analysis. The first analysis proves that if an integrator backstepping signal is square integrable then the link position is globally uniformly bounded (GUB). The second analysis proves that the backstepping signal is square integrable, all the system states are bounded, and that the velocity field tracking error converges to zero despite parametric uncertainty in the dynamic model. A numerical simulation based on the velocity field presented in [5] is provided to demonstrate the performance of the VFC approach. In Section 4, a navigation function based trajectory planning and control development is presented, along with the stability analysis. This analysis proves that the backstepping signal is square integrable, all the system states are bounded, and that the robot end-effector will track an obstacle free path to a goal point, despite parametric uncertainty in the dynamic model. A numerical simulation for the adaptive navigation function controller is provided to demonstrate the performance of the approach. Concluding remarks are provided in Section 5.

2 System Model

The mathematical model for an n -DOF robotic manipulator is assumed to have the following form

$$M(q)\ddot{q} + V_m(q, \dot{q})\dot{q} + G(q) = \tau. \quad (3)$$

²A continuous function $\alpha : [0, \alpha) \rightarrow [0, \infty)$ is said to belong to class \mathcal{K} if it is strictly increasing and $\alpha(0) = 0$ [13].

In (3), $q(t)$, $\dot{q}(t)$, $\ddot{q}(t) \in \mathbb{R}^n$ denote the joint position, velocity, and acceleration, respectively, $M(q) \in \mathbb{R}^{n \times n}$ represents the positive-definite, symmetric inertia matrix, $V_m(q, \dot{q}) \in \mathbb{R}^{n \times n}$ represents the centripetal-Coriolis terms, $G(q) \in \mathbb{R}^n$ represents the known gravitational vector, and $\tau(t) \in \mathbb{R}^n$ represents the joint torque input vector. We will assume that $q(t)$ and $\dot{q}(t)$ are measurable. The dynamic model in (3), exhibits the following properties that are utilized in the subsequent control development and stability analysis.

Property 1: The inertia matrix can be upper and lower bounded by the following inequalities [1]

$$m_1 \|\xi\|^2 \leq \xi^T M(q)\xi \leq m_2(q) \|\xi\|^2 \quad \forall \xi \in \mathbb{R}^n \quad (4)$$

where m_1 is a positive constant, $m_2(\cdot)$ is a positive function, and $\|\cdot\|$ denotes the Euclidean norm.

Property 2: The inertia and the centripetal-Coriolis matrices satisfy the following relationship [1]

$$\xi^T \left(\frac{1}{2} \dot{M}(q) - V_m(q, \dot{q}) \right) \xi = 0 \quad \forall \xi \in \mathbb{R}^n \quad (5)$$

where $\dot{M}(q)$ represents the time derivative of the inertia matrix.

Property 3: The robot dynamics given in (3) can be linearly parameterized as follows [1]

$$Y(q, \dot{q}, \ddot{q})\theta \triangleq M(q)\ddot{q} + V_m(q, \dot{q})\dot{q} + G(q) \quad (6)$$

where $\theta \in \mathbb{R}^p$ contains constant system parameters, and $Y(q, \dot{q}, \ddot{q}) \in \mathbb{R}^{n \times p}$ denotes a regression matrix composed of $q(t)$, $\dot{q}(t)$, and $\ddot{q}(t)$.

3 Adaptive VFC

3.1 Control Objective

As described previously, many robotic tasks can be effectively encapsulated as a velocity field. That is, the velocity field control objective can be described as commanding the robot end-effector to track a velocity field that is defined as a function of the current joint position. To quantify this objective, a velocity field tracking error, denoted by $\eta_1(t) \in \mathbb{R}^n$, is defined as follows

$$\eta_1(t) \triangleq \dot{q}(t) - \vartheta(q) \quad (7)$$

where $\vartheta(\cdot) \in \mathbb{R}^n$ denotes the velocity field. To achieve the control objective, the subsequent development is based on the assumption that $q(t)$ and $\dot{q}(t)$ are measurable, and that $\vartheta(q)$ and its partial derivative $\frac{\partial \vartheta(q)}{\partial q} \in \mathbb{R}^n$, are assumed to be bounded provided $q(t) \in \mathcal{L}_\infty$.

3.2 Benchmark Control Modification

To develop the open-loop error dynamics for $\eta_1(t)$, we take the time derivative of (7) and premultiply the resulting expression by the inertia matrix as follows

$$\begin{aligned} M(q)\dot{\eta}_1 &= -V_m(q, \dot{q})\dot{q} - G(q) + \tau + V_m(q, \dot{q})\vartheta(q) \\ &\quad - V_m(q, \dot{q})\vartheta(q) - M(q)\frac{\partial \vartheta(q)}{\partial q}\dot{q} \end{aligned} \quad (8)$$

where (3) was utilized. From (5) and (7), the expression in (8) can be rewritten as follows

$$M(q)\dot{\eta}_1 = -V_m(q, \dot{q})\eta_1 - Y_1(q, \dot{q})\theta + \tau \quad (9)$$

where θ was introduced in (6) and $Y_1(q, \dot{q}) \in \mathbb{R}^{n \times p}$ denotes a measurable regression matrix that is defined as follows

$$Y_1(q, \dot{q})\theta \triangleq M(q)\frac{\partial \vartheta(q)}{\partial q}\dot{q} + V_m(q, \dot{q})\vartheta(q) + G(q). \quad (10)$$

Based on the open-loop error system in (9), a number of control designs could be utilized to ensure velocity field tracking (i.e., $\|\eta_1(t)\| \rightarrow 0$) given the assumption in (1). Motivated by the desire to eliminate the assumption in (1), a norm squared gradient term is incorporated in an adaptive controller introduced in [24] as follows

$$\tau(t) \triangleq - \left(K + \left\| \frac{\partial V(q)}{\partial q} \right\|^2 \right) \eta_1 + Y_1(q, \dot{q})\hat{\theta}_1 \quad (11)$$

where $K \in \mathbb{R}^{n \times n}$ is a constant, positive definite diagonal matrix, and $\frac{\partial V(q)}{\partial q}$ was introduced in (2). In (11), $\hat{\theta}_1(t) \in \mathbb{R}^p$ denotes a parameter estimate that is generated by the following gradient update law

$$\dot{\hat{\theta}}_1(t) = -\Gamma_1 Y_1^T(q, \dot{q})\eta_1 \quad (12)$$

where $\Gamma_1 \in \mathbb{R}^{p \times p}$ is a constant, positive definite diagonal matrix. After substituting (11) into (9), the following closed-loop error system can be obtained

$$M(q)\dot{\eta}_1 = -V_m(q, \dot{q})\eta_1 - Y_1(q, \dot{q})\tilde{\theta}_1 - \left(K + \left\| \frac{\partial V(q)}{\partial q} \right\|^2 \right) \eta_1 \quad (13)$$

where the parameter estimation error signal $\tilde{\theta}_1(t) \in \mathbb{R}^p$ is defined as follows

$$\tilde{\theta}_1(t) \triangleq \theta - \hat{\theta}_1. \quad (14)$$

Remark 1 While the control development is based on a modification of the adaptive controller introduced in [24], the norm squared gradient term could also be incorporated in other benchmark controllers to yield similar results.

3.3 Stability Analysis

To facilitate the subsequent stability analysis, the following preliminary theorem is utilized.

Theorem 1 Let $\bar{V}(t) \in \mathbb{R}$ denote the following nonnegative, continuous differentiable function

$$\bar{V}(t) \triangleq V(q) + P(t) \quad (15)$$

where $V(q) \in \mathbb{R}$ denotes a nonnegative, continuous differentiable function that satisfies (2) and the following inequalities

$$0 \leq \gamma_1(q) \leq V(q) \leq \gamma_2(q) \quad (16)$$

where $\gamma_1(\cdot), \gamma_2(\cdot)$ are class \mathcal{K} functions, and $P(t) \in \mathbb{R}$ denotes the following nonnegative, continuous differentiable function

$$P(t) \triangleq \gamma - \int_{t_0}^t \varepsilon^2(\sigma) d\sigma \quad (17)$$

where $\gamma \in \mathbb{R}$ is a positive constant, and $\varepsilon(t) \in \mathbb{R}$ is defined as follows

$$\varepsilon \triangleq \left\| \frac{\partial V(q)}{\partial q} \right\| \|\eta_1\|. \quad (18)$$

If $\varepsilon(t)$ is a square integrable function, where

$$\int_{t_0}^t \varepsilon^2(\sigma) d\sigma \leq \gamma, \quad (19)$$

and if after utilizing (7), the time derivative of $\bar{V}(t)$ satisfies the following inequality

$$\dot{\bar{V}}(t) \leq -\gamma_3(q) + \xi_0 \quad (20)$$

where $\gamma_3(q)$ is the class \mathcal{K} function introduced in (2), and $\xi_0 \in \mathbb{R}$ denotes a positive constant, then $q(t)$ is global uniformly bounded.

Proof: The time derivative of $\bar{V}(t)$ can be expressed as follows

$$\dot{\bar{V}}(t) = \frac{\partial V(q)}{\partial q} \vartheta(q) + \frac{\partial V(q)}{\partial q} \eta_1 - \varepsilon^2(t)$$

where (7) and (17) were utilized. By exploiting the assumption introduced in (2) and the definition for $\varepsilon(t)$ provided in (18), the following inequality can be obtained

$$\dot{\bar{V}}(t) \leq -\gamma_3(q) + \zeta_0 + [\varepsilon(t) - \varepsilon^2(t)]. \quad (21)$$

After completing the squares on the bracketed terms in (21), the inequality introduced in (20) is obtained where

$$\xi_0 \triangleq \zeta_0 + \frac{1}{4}.$$

Hence, if $\varepsilon(t) \in \mathcal{L}_2$, then Lemma 1 in the appendix can be used to prove that $q(t)$ is GUB. ■

In the following analysis, we first prove that $\varepsilon(t) \in \mathcal{L}_2$. Based on the conclusion that $\varepsilon(t) \in \mathcal{L}_2$, the result from Theorem 1 is utilized to ensure that $q(t)$ is bounded under the proposed adaptive controller given in (11) and (12).

Theorem 2 *The adaptive VFC given in (11) and (12) yields global velocity field tracking in the sense that*

$$\|\eta_1(t)\| \rightarrow 0. \quad (22)$$

Proof: Let $V_1(t) \in \mathbb{R}$ denote the following nonnegative function

$$V_1 \triangleq \frac{1}{2} \eta_1^T M \eta_1 + \frac{1}{2} \tilde{\theta}_1^T \Gamma_1^{-1} \tilde{\theta}_1. \quad (23)$$

After taking the time derivative of (23) the following expression can be obtained

$$\dot{V}_1 = -\eta^T \left(Y_1(q, \dot{q}) \tilde{\theta}_1 + \left(K + \left\| \frac{\partial V(q)}{\partial q} \right\|^2 \right) \eta_1 \right) - \tilde{\theta}_1^T \Gamma_1^{-1} \dot{\tilde{\theta}}_1 \quad (24)$$

where (5) and (13) were utilized. After utilizing the parameter update law given in (12), the expression given in (24) can be rewritten as follows

$$\dot{V}_1 = -\eta_1^T \left(K + \left\| \frac{\partial V(q)}{\partial q} \right\|^2 \right) \eta_1. \quad (25)$$

The expressions given in (18), (23), and (25) can be used to conclude that $\eta_1(t), \tilde{\theta}_1(t) \in \mathcal{L}_\infty$ and $\eta_1(t), \varepsilon(t) \in \mathcal{L}_2$. From the fact that $\tilde{\theta}_1(t) \in \mathcal{L}_\infty$, (14) can be used to prove that $\theta_1(t) \in \mathcal{L}_\infty$. Based on the fact that $\varepsilon(t) \in \mathcal{L}_2$, the results from Theorem 1 can be used to prove that $q(t) \in \mathcal{L}_\infty$. Based on the fact that $q(t), \eta_1(t) \in \mathcal{L}_\infty$ and the assumption that $\vartheta(q), \frac{\partial V(q)}{\partial q} \in \mathcal{L}_\infty$ provided $q(t) \in \mathcal{L}_\infty$, the expressions in (7) and (18) can be used to prove that $\dot{q}(t), \varepsilon(t) \in \mathcal{L}_\infty$. Based on these facts, the expressions given in (10)-(13) can be used to prove that $Y_1(q, \dot{q}), \tau(t), \dot{\theta}_1(t), \dot{\eta}_1(t) \in \mathcal{L}_\infty$. Given that $\eta_1(t), \dot{\eta}_1(t) \in \mathcal{L}_\infty$ and $\eta_1(t) \in \mathcal{L}_2$, Barbalat's Lemma [24] can now be utilized to prove (22). ■

3.4 Numerical Simulation

A numerical simulation was performed to demonstrate the performance of the adaptive VFC given in (11) and (12). For this simulation, a velocity field for a planar, circular task-space contour was selected to satisfy the assumption given in (2). Specifically, the following contour was utilized [5]

$$\vartheta(x) = -K(x)f(x) \begin{bmatrix} 2(x_1 - x_{c1}) \\ 2(x_2 - x_{c2}) \end{bmatrix} + c(x) \begin{bmatrix} -2(x_2 - x_{c2}) \\ 2(x_1 - x_{c1}) \end{bmatrix}. \quad (26)$$

In (26), $x_{c1} = 0.318[\text{m}]$ and $x_{c2} = 0.318[\text{m}]$ denote the circle center, and the functions $f(x)$, $K(x)$, and $c(x) \in \mathbb{R}$ are defined as follows

$$\begin{aligned} f(x) &= (x_1 - x_{c1})^2 + (x_2 - x_{c2})^2 - r_o^2 \\ K(x) &= \frac{k_0^*}{\sqrt{f^2(x)} \left\| \frac{\partial f(x)}{\partial x} \right\| + \epsilon} \\ c(x) &= \frac{c_0 \exp\left(-\mu \sqrt{f^2(x)}\right)}{\left\| \frac{\partial f(x)}{\partial x} \right\|} \end{aligned} \quad (27)$$

where $r_o = 0.2[\text{m}]$ denotes the circle diameter; $\epsilon = 0.005[\text{m}^3]$ and $\mu = 20[\text{m}^{-1}]$ are auxiliary parameters; and $k_0^* = 0.1[\text{ms}^{-1}]$ and $c_0 = 0.1[\text{ms}^{-1}]$ are tracking speed parameters. Values for the above parameters were chosen based on the velocity field presented in [5].

The two link robot presented in [5] was used for this control problem with the following forward kinematics

$$\begin{bmatrix} x_1 \\ x_2 \end{bmatrix} = \begin{bmatrix} \ell_1 \sin(q_1) + \ell_2 \sin(q_2 + q_1) \\ -\ell_1 \cos(q_1) - \ell_2 \cos(q_1 + q_2) \end{bmatrix} \quad (28)$$

and manipulator Jacobian

$$J(q) = \begin{bmatrix} \ell_1 \cos(q_1) + \ell_2 \cos(q_1 + q_2) & \ell_2 \cos(q_1 + q_2) \\ \ell_1 \sin(q_1) + \ell_2 \sin(q_2 + q_1) & \ell_2 \sin(q_2 + q_1) \end{bmatrix}. \quad (29)$$

In (28) and (29), the robot link lengths denoted by $\ell_1 = \ell_2 = 0.45[\text{m}]$. From (26)-(29) the joint-space velocity field can be determined as follows $\vartheta(q) = J^{-1}(q)\vartheta(x)$. The initial conditions of the system were selected as $q(0) = \dot{q}(0) = 0$. The control gains were adjusted to the following values

$$K = \text{diag}(200, 200) \quad \Gamma = \text{diag}(2, 1, 1, 1000, 500)$$

where $diag(\cdot)$ denotes a diagonal matrix with the arguments as the diagonal entries. Figures 1-3 depict the velocity field tracking error, the parameter estimates, and the control torque inputs, respectively.

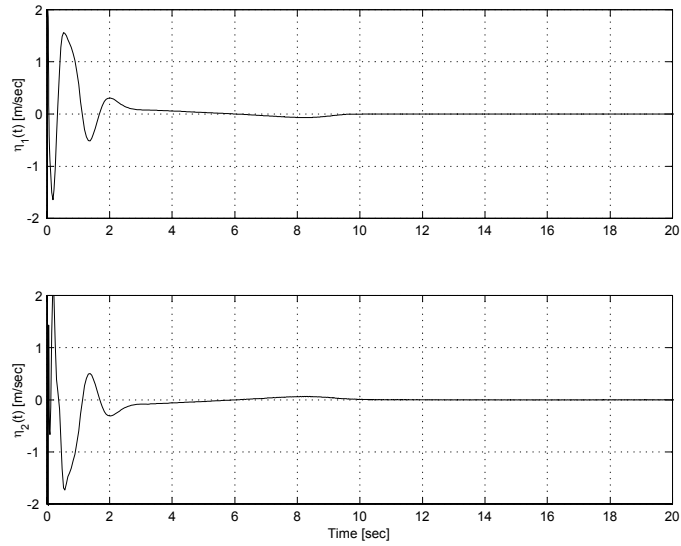


Figure 1: Velocity field tracking error.

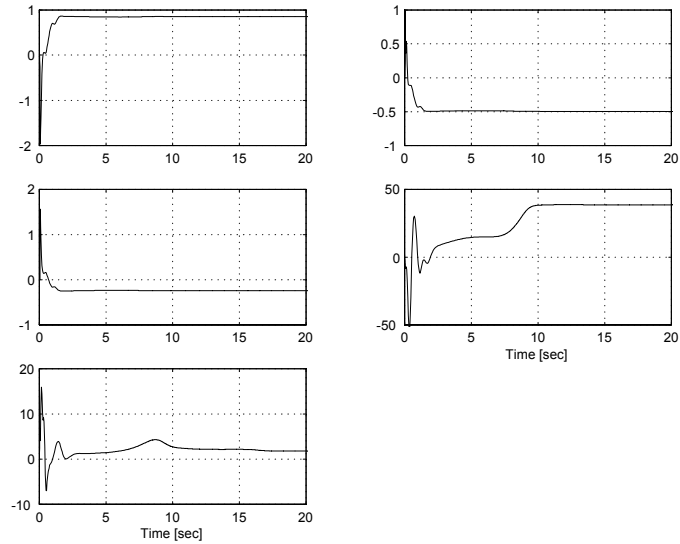


Figure 2: Parameter estimates.

4 Navigation Function Control Extension

4.1 Control Objective

The objective in this extension is to navigate a robot end-effector along a collision-free path to a constant goal point, denoted by $q^* \in \mathcal{D}$, where the set \mathcal{D} denotes a free configuration space that is

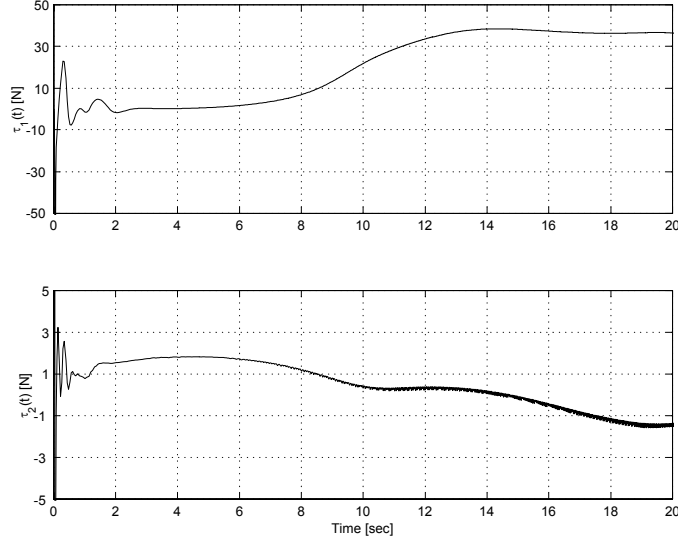


Figure 3: Control torque.

a subset of the whole configuration space with all configurations removed that involve a collision with an obstacle. Mathematically, the control objective can be stated as the desire to ensure that

$$q(t) \rightarrow q^* \quad (30)$$

where another objective of the trajectory planner and the controller is to ensure that $q(t) \in \mathcal{D}$. To generate the reference trajectory, the special artificial potential function coined a navigation function in [17], can be used. Specifically, the navigation functions used in this paper are defined as follows [23].

Definition: A map $\varphi(\cdot) : \mathcal{D} \rightarrow [0, 1]$, is a navigation function if $\varphi(\cdot)$:

- 1) is analytic on \mathcal{D} (at least the first and second partial derivatives exist and are bounded on \mathcal{D});
- 2) has a unique minimum at q^* ;
- 3) obtains a maximum value on the boundary of \mathcal{D} (i.e., admissible on \mathcal{D});
- 4) is a Morse function (i.e., the matrix of second partial derivatives, the Hessian, evaluated at its critical points is nonsingular (and has bounded elements based on the smoothness property in part 1)).
- 5) From Property 1) and Property 2), it is clear when the gradient vector $\varphi(\xi) \rightarrow 0$ that $\xi \rightarrow q^*$.

Based on (30) and the definition of a navigation function, a navigation function tracking error, denoted by $\eta_2(t) \in \mathbb{R}^n$, can be defined as follows to quantify the control objective

$$\eta_2(t) \triangleq \dot{q}(t) + \nabla\varphi(q) \quad (31)$$

where $\varphi(q) \in \mathbb{R}$ denotes a navigation function defined in the set \mathcal{D} , and $\nabla\varphi(q)$ denotes the gradient vector of $\varphi(q)$ defined as follows

$$\nabla\varphi(q) \triangleq \left[\frac{\partial\varphi}{\partial q_1} \quad \frac{\partial\varphi}{\partial q_2} \quad \dots \quad \frac{\partial\varphi}{\partial q_n} \right]^T. \quad (32)$$

4.2 Benchmark Control Modification

To develop the open-loop error dynamics for $\eta_2(t)$, we take the time derivative of (31) and premultiply the resulting expression by the inertia matrix as follows

$$M\dot{\eta}_2 = -V_m(q, \dot{q})\eta_2 + Y_2(q, \dot{q})\theta + \tau. \quad (33)$$

where (3) and (31) were utilized. In (33), the linear parameterization $Y_2(q, \dot{q})\theta$ is defined as follows

$$Y_2(q, \dot{q})\theta \triangleq M(q)f(q, \dot{q}) + V_m(q, \dot{q}) \nabla \varphi(q) - G(q) \quad (34)$$

where $Y_2(q, \dot{q}) \in \mathbb{R}^{n \times m}$ denotes a measurable regression matrix, $\theta \in \mathbb{R}^m$ was introduced in (6), and the auxiliary signal $f(q, \dot{q}) \in \mathbb{R}^n$ is defined as

$$f(q, \dot{q}) \triangleq \frac{d}{dt} (\nabla \varphi(q)). \quad (35)$$

Based on (33) and the subsequent stability analysis, the following adaptive controller introduced in [24] can be utilized

$$\tau \triangleq -k\eta_2 - Y_2(q, \dot{q})\hat{\theta}_2 \quad (36)$$

where $k \in \mathbb{R}$ is a positive constant gain, and $\hat{\theta}_2(t) \in \mathbb{R}^p$ denotes a parameter update law that is generated from the following expression

$$\dot{\hat{\theta}}_2(t) \triangleq -\Gamma_2 Y_2^T(q, \dot{q})\eta_2 \quad (37)$$

where $\Gamma_2 \in \mathbb{R}^{m \times m}$ is a positive definite, diagonal gain matrix. Note that the trajectory planning is incorporated in the controller through the gradient terms included in (34) and (35). After substituting (36) into (33) the following closed loop error systems can be obtained

$$M\dot{\eta}_2 = -V_m(q, \dot{q})\eta_2 - k\eta_2 + Y_2(q, \dot{q})\tilde{\theta}_2 \quad (38)$$

where $\tilde{\theta}_2(t) \in \mathbb{R}^p$ is defined as follows

$$\tilde{\theta}_2(t) \triangleq \theta - \hat{\theta}_2. \quad (39)$$

4.3 Stability Analysis

Theorem 3 *The adaptive controller given in (36) and (37) ensures that the robot end-effector tracks an obstacle free path to the unique goal point in sense that*

$$\nabla \varphi(q) \rightarrow 0 \implies q(t) \rightarrow q^* \text{ as } t \rightarrow \infty \quad (40)$$

provided the following sufficient condition is satisfied

$$k > \frac{2}{\gamma} \quad (41)$$

where $\gamma \in \mathbb{R}$ is an adjustable constant.

Proof: Let $V_2(q, \eta_2, \tilde{\theta}_2) \in \mathbb{R}$ denote the following nonnegative function

$$V_2 \triangleq \varphi(q) + \gamma \left[\frac{1}{2} \eta_2^T M \eta_2 + \tilde{\theta}_2^T \Gamma_2^{-1} \tilde{\theta}_2 \right]. \quad (42)$$

After taking the time derivative of (42) the following expression can be obtained

$$\dot{V}_2 = [\nabla \varphi(q)]^T \dot{q} + \gamma \eta_2^T \left(-k \eta_2 + Y_2(q, \dot{q}) \tilde{\theta}_2 - \tilde{\theta}_2^T \Gamma_2^{-1} \dot{\tilde{\theta}}_2 \right) \quad (43)$$

where (5), (32), (38), and (39) were utilized. By utilizing (31), (37), and the triangle inequality, the following expression can be obtained

$$\dot{V}_2 \leq -\frac{1}{2} \|\nabla \varphi(q)\|^2 - (\gamma k - 2) \|\eta_2\|^2. \quad (44)$$

Provided k and γ are selected to satisfy the sufficient condition introduced in (41), it is clear from (4), (42), and (44) that

$$0 \leq \varphi(q(t)) + \gamma \zeta(q, t) \leq |\varphi(q(0))| + \gamma \zeta(q(0), 0) \quad (45)$$

where $\zeta(q, t) \in \mathbb{R}$ is defined as

$$\zeta(q, t) \triangleq \left[\frac{m_2(q)}{2} \|\eta_2(t)\|^2 + \lambda_{\max}\{\Gamma_2^{-1}\} \|\tilde{\theta}_2(t)\|^2 \right]. \quad (46)$$

From (39), (45), and (46) it is clear that $\eta_2(t)$, $\varphi(q)$, $\tilde{\theta}_2(t)$, $\hat{\theta}_2(t) \in \mathcal{L}_\infty$. Based on Property 1 of the definition of a navigation function, $\nabla \varphi(q) \in \mathcal{L}_\infty$. Since $\eta_2(t)$, $\nabla \varphi(q) \in \mathcal{L}_\infty$, (31) can be used to conclude that $\dot{q}(t) \in \mathcal{L}_\infty$; hence, Property 1 of the definition of a navigation function and (35) can be used to conclude that $f(q, \dot{q}) \in \mathcal{L}_\infty$. Based on the previous boundedness statements, (34) can be used to show that $Y_2(q, \dot{q}, q^*) \in \mathcal{L}_\infty$; hence, (36) and (37) can be used to prove that $\tau(t)$, $\dot{\hat{\theta}}_2(t) \in \mathcal{L}_\infty$. From (44), it can also be determined that $\nabla \varphi(q)$, $\eta_2(t) \in \mathcal{L}_2$. From the fact that $\nabla \varphi(q) \in \mathcal{L}_\infty \cap \mathcal{L}_2$, Barbalat's lemma [24] can be used to show that $\nabla \varphi(q) \rightarrow 0$. Since $\nabla \varphi(q) \rightarrow 0$, Property 5 of the definition of a navigation function can be used to prove that $q(t) \rightarrow q^*$ as $t \rightarrow \infty$.

Based on (45) and (46), it is clear that to ensure that $q(t)$ will remain in \mathcal{D} , the free configuration space must be sized to account for the effects of $\gamma \zeta(q(0), 0)$. To minimize the effects of $\gamma \zeta(q(0), 0)$, the initial conditions $\eta_2(0)$ and $\tilde{\theta}_2(0)$ could be required to be sufficiently small, and γ can be selected arbitrarily small. ■

4.4 Numerical Simulation

To illustrate the performance of the controller given in (37) and (36), a numerical simulation was performed to navigate a two link robot from its initial position to the task-space goal point, denoted by $x^* \triangleq [x_1^*, x_2^*]^T \in \mathbb{R}^2$. The same forward kinematic and Jacobian as defined in (28) and (29) are utilized along with the dynamic model given in (3). A task-space potential function $\varphi(x)$ is chosen as follows

$$\varphi(x) = \frac{\|x - x^*\|^2}{(\|x - x^*\|^{2\kappa} + \beta_0 \beta_1 \beta_2 \beta_3 \beta_4)^{1/\kappa}} \quad (47)$$

where $x(t) \triangleq [x_1(t), x_2(t)]^T \in \mathbb{R}^2$. In (47), $\kappa \in \mathbb{R}$ denotes some positive integer. If κ is selected large enough, it is proven in [17] that $\varphi(x, x^*)$ is a navigation function for $x(t)$. In (47), the boundary function $\beta_0(x) \in \mathbb{R}$ and the obstacle functions $\beta_1(x), \beta_2(x), \beta_3(x), \beta_4(x) \in \mathbb{R}$ are defined as follows

$$\begin{aligned}\beta_0 &= r_0^2 - (x_1 - x_{1r_0})^2 - (x_2 - x_{2r_0})^2 \\ \beta_1 &= (x_1 - x_{r_1})^2 + (x_2 - x_{2r_1})^2 - r_1^2 \\ \beta_2 &= (x_1 - x_{r_2})^2 + (x_2 - x_{2r_2})^2 - r_2^2 \\ \beta_3 &= (x_1 - x_{r_3})^2 + (x_2 - x_{2r_3})^2 - r_3^2 \\ \beta_4 &= (x_1 - x_{r_4})^2 + (x_2 - x_{2r_4})^2 - r_4^2.\end{aligned}\tag{48}$$

In (48), $(x_1 - x_{1r_i})$ and $(x_2 - x_{2r_i})$ where $i = 0, 1, 2, 3, 4$ are the centers of the boundary and obstacles respectively, $r_0, r_1, r_2, r_3, r_4 \in \mathbb{R}$ are the radii of the boundary and obstacles respectively. From (47) and (48) it is clear that model space is a circle that excludes four circles described by the obstacle functions $\beta_1(x), \beta_2(x), \beta_3(x), \beta_4(x)$. For this simulation the model-space configuration [17] is selected as follows

$$\begin{aligned}x_{1r_0} &= 0.41 & x_{2r_0} &= -0.41 & r_0 &= 0.4 \\ x_{1r_1} &= 0.55 & x_{2r_1} &= -0.25 & r_1 &= 0.05 \\ x_{1r_2} &= 0.25 & x_{2r_2} &= -0.25 & r_2 &= 0.05 \\ x_{1r_3} &= 0.25 & x_{2r_3} &= -0.55 & r_3 &= 0.05 \\ x_{1r_4} &= 0.55 & x_{2r_4} &= -0.55 & r_4 &= 0.05.\end{aligned}$$

Since the navigation function in the simulation is defined in the task-space, (28) and (29) can be used to design the control in the task-space.

The control gains were adjusted to the following values to yield the best performance

$$\begin{aligned}\kappa &= 6 & k &= 100 \\ \Gamma_2 &= \text{diag}(100, 100, 100, 100, 100).\end{aligned}$$

The actual trajectory of the two link robot can be seen in Figure 4. The outer circle in Figure 4 depicts the outer boundary of the model space. The four inner circles in Figure 4 depicts the obstacle that are to be avoided. Figure illustrates that the end-effector avoids the obstacles as it moves to the goal point. The parameter estimates and control torque are provided in Figures 5 and 6, respectively.

5 Conclusion

Two trajectory planning and adaptive tracking controllers are presented. The benchmark adaptive tracking controller by Slotine [24] was modified to achieve velocity field tracking in the presence of parametric uncertainty in the robot dynamics. By incorporating a norm squared gradient term the VFC, the boundedness of all signals can be proven without the typical assumption that bounds the integral of the velocity field. An extension was then provided that also modifies a standard adaptive controller by incorporating a gradient based term. Using standard backstepping techniques, a Lyapunov analysis was used to prove that a navigation function could be incorporated in the control design to ensure the robot remained on an obstacle free path within an expanded configuration space to reach a goal configuration. Simulation results illustrated the performance of the tracking controller and the on-line path planning capabilities of the controller.

Figure 4: Actual trajectory of the Two Link Robot

Figure 5: Parameter update estimates.

Figure 6: Control torque.

References

- [1] F. Lewis, C. Abdallah, and D. Dawson, *Control of Robot Manipulators*, New York: MacMillan Publishing Co., 1993.
- [2] A. Bemporad, A. De Luca, and G. Oriolo, "Local Incremental Planning for a Car-Like Robot Navigating Among Obstacles," *Proc. of the IEEE International Conference on Robotics and Automation*, Minneapolis, Minnesota, pp. 1205-1211, April 1996.
- [3] J. Barraquand and J. C. Latombe, "A Monte-Carlo Algorithm for Path Planning with Many Degrees of Freedom," *Proc. of the IEEE International Conference on Robotics and Automation*, Cincinnati, Ohio, pp. 584-589, May 1990.
- [4] J. Barraquand, B. Langlois, and J. C. Latombe, "Numerical Potential Fields Techniques for Robot Path Planning," *IEEE Transactions on Systems, Man, and Cybernetics*, Vol. 22, pp. 224-241, (1992).
- [5] I. Cervantes, R. Kelly, J. Alvarez-Ramirez, and J. Moreno, "A Robust Velocity Field Control," *IEEE Transactions on Control Systems Technology*, Vol. 10, No. 6, pp. 888-894, (2002).
- [6] C. I. Connolly, J. B. Burns, and R. Weiss, "Path Planning Using Laplace's Equation," *Proc. of the IEEE International Conference on Robotics and Automation*, Cincinnati, Ohio, pp. 2102-2106, May 1990.
- [7] M.S. de Queiroz, D.M. Dawson, S.P. Nagarkatti, and F. Zhang, *Lyapunov-Based Control of Mechanical Systems*, Birkhäuser, 1999.
- [8] W. E. Dixon, D. M. Dawson, E. Zergeroglu, and F. Zhang, "Robust Tracking and Regulation Control for Mobile Robots," *International Journal of Robust and Nonlinear Control*, Vol. 10, pp. 199-216, (2000).

- [9] W. E. Dixon, D. M. Dawson, E. Zergeroglu, and A. Behal, *Nonlinear Control of Wheeled Mobile Robots*, Springer-Verlag London Limited, 2001.
- [10] S. S. Ge and Y. J. Cui, "New Potential Functions for Mobile Robot Path Planning," *IEEE Transactions on Robotics and Automation*, Vol. 16, No. 5, pp. 615-620, (2000).
- [11] J. Guldner and V. I. Utkin, "Sliding Mode Control for Gradient Tracking and Robot Navigation Using Artificial Potential Fields," *IEEE Transactions on Robotics and Automation*, Vol. 11, No. 2, pp. 247-254, (1995).
- [12] J. Guldner, V. I. Utkin, H. Hashimoto, and F. Harashima, "Tracking Gradients of Artificial Potential Field with Non-Holonomic Mobile Robots," *Proc. of the American Control Conference*, Seattle, Washington, pp. 2803-2804, June 1995.
- [13] H. K. Khalil, *Nonlinear Systems*, third edition, Prentice Hall, 2002.
- [14] O. Khatib, *Commande dynamique dans l'espace opérationnel des robots manipulateurs en présence d'obstacles*, Ph.D. Dissertation, École Nationale Supérieure de l'Aéronautique et de l'Espace (ENSAE), France, 1980.
- [15] O. Khatib, "Real-Time Obstacle Avoidance for Manipulators and Mobile Robots," *International Journal of Robotics Research*, Vol. 5, No. 1, pp. 90-99, (1986).
- [16] K. J. Kyriakopoulos, H. G. Tanner, and N. J. Krikelis, "Navigation of Nonholonomic Vehicles in Complex Environments with Potential Fields and Tracking," *Int. J. Intell. Contr. Syst.*, Vol. 1, No. 4, pp. 487-495, (1996).
- [17] D. E. Koditschek, "Exact Robot Navigation by Means of Potential Functions: Some Topological Considerations," *Proc. of the IEEE International Conference on Robotics and Automation*, Raleigh, North Carolina, pp. 1-6, May 1987.
- [18] D. E. Koditschek and E. Rimon, "Robot Navigation Functions on Manifolds with Boundary," *Adv. Appl. Math.*, Vol. 11, pp. 412-442, (1990).
- [19] J. P. Laumond, P. E. Jacobs, M. Taix, and R. M. Murray, "A Motion Planner for Nonholonomic Mobile Robots," *IEEE Transactions on Robotics and Automation*, Vol. 10, No. 5, pp. 577-593, (1994).
- [20] J. C. Latombe, *Robot Motion Planning*, Kluwer Academic Publishers: Boston, Massachusetts, 1991.
- [21] P. Li and R. Horowitz, "Passive Velocity Field Control of Mechanical Manipulators," *IEEE Transactions on Robotics and Automation*, Vol. 15, No. 4, pp. 751-763, (2003).
- [22] A. De Luca and G. Oriolo, "Local Incremental Planning for Nonholonomic Mobile Robots," *Proc. of the IEEE International Conference on Robotics and Automation*, San Diego, California, pp. 104-110, May 1994.
- [23] E. Rimon and D. E. Koditschek, "Exact Robot Navigation Using Artificial Potential Function," *IEEE Transactions on Robotics and Automation*, Vol. 8, No. 5, pp. 501-518, (1992).
- [24] J.J.E. Slotine and W. Li, *Applied Nonlinear Control*, Englewood Cliff, NJ: Prentice Hall, Inc., 1991.

- [25] H. G. Tanner and K. J. Kyriakopoulos, “Nonholonomic Motion Planning for Mobile Manipulators,” *Proc. of the IEEE International Conference on Robotics and Automation*, San Francisco, California, pp. 1233-1238, April 2000.
- [26] H. G. Tanner, S. G. Loizou, and K. J. Kyriakopoulos, “Nonholonomic Navigation and Control of Cooperating Mobile Manipulators,” *IEEE Transactions on Robotics and Automation*, Vol. 19, No. 1, pp. 53-64, (2003).
- [27] R. Volpe and P. Khosla, “Artificial Potential with Elliptical Isopotential Contours for Obstacle Avoidance,” *Proc. of the IEEE Conference on Decision and Control*, Los Angeles, California, pp. 180-185, December 1987.
- [28] E. W. Weisstein, *CRC Concise Encyclopedia of Mathematics*, Second Edition, CRC Press, 2002.
- [29] D. Lee and P. Li, “Passive Bilateral Feedforward Control of Linear Dynamically Similar Teleoperated Manipulators,” *IEEE Transactions on Robotics and Automation*, Vol. 19, No. 3, pp. 443-456 (2003).
- [30] J. Li and P. Li, “Passive Velocity Field Control (PVFC) Approach to Robot Force Control and Contour Following,” *Proc. of the Japan/USA Symposium on Flexible Automation*, Ann Arbor, Michigan, July 2000.
- [31] Y. Nakamura, *Advanced Robotics Redundancy and Optimization*, Addison-Wesley, 1991.
- [32] Z. Qu, *Robust Control of Nonlinear Uncertain Systems*, New York: John Wiley & Sons, 1998.
- [33] M. Yamakita, T. Yazawa, X.-Z. Zheng, and K. Ito, “An Application of Passive Velocity Field Control to Cooperative Multiple 3-Wheeled Mobile Robots,” *Proceedings of the IEEE/RJS International Conference on Intelligent Robots and Systems*, Victoria, B. C., Canada, pp. 368-373, October 1998.
- [34] M. Yamakita, K. Suzuki, X.-Z. Zheng, M. Katayama, and K. Ito, “An Extension of Passive Velocity Field Control to Cooperative Multiple Manipulator Systems,” *Proc. of the IEEE/RJS International Conference on Intelligent Robots and Systems*, Grenoble, France, pp. 11-16, October 1997.

Appendix

Lemma 1 *Given a continuously differentiable function, denoted by $V(q)$, that satisfies the following inequalities*

$$0 < \gamma_1(q) \leq V(q) \leq \gamma_2(q) + \xi_b \quad (49)$$

with a time derivative that satisfies the following inequality

$$\dot{V}(q) \leq -\gamma_3(q) + \xi_0, \quad (50)$$

then $q(t)$ is GUB, where $\gamma_1(\cdot)$, $\gamma_2(\cdot)$, $\gamma_3(\cdot)$ are class \mathcal{K} functions, and $\xi_0, \xi_b \in \mathbb{R}$ denote positive constants.

Proof:³ Let $\Omega \in \mathbb{R}$ be a positive function defined as follows

$$\Omega \triangleq \gamma_3^{-1}(\xi_0) > 0 \quad (51)$$

where $\gamma_3^{-1}(\cdot)$ denotes the inverse of $\gamma_3(\cdot)$, and let $B(0, \Omega)$ denote a ball centered about the origin with a radius of Ω . Consider the following 2 possible cases.

The initial condition $q(t_0)$ lies outside the ball $B(0, \Omega)$ as follows

$$\Omega < \|q(t_0)\| \leq \Omega_1 \quad (52)$$

where $\Omega_1 \in \mathbb{R}$ is a positive constant. To facilitate further analysis, we define the operator $d(\cdot)$ as follows

$$d(\Omega_1) \triangleq (\gamma_1^{-1} \circ \gamma_2)(\Omega_1) + \gamma_1^{-1}(\xi_b) > 0 \quad (53)$$

where $(\gamma_1^{-1} \circ \gamma_2)$ denotes the composition of the inverse of $\gamma_1(\cdot)$ with $\gamma_2(\cdot)$ (i.e., the inverse of the function $\gamma_1(\cdot)$ is applied to the function $\gamma_2(\cdot)$). After substituting the constant $d(\Omega_1)$ into $\gamma_1(\cdot)$, the following inequalities can be determined

$$\gamma_1(d\Omega_1) = \gamma_2(\Omega_1) + \xi_b \geq \gamma_2(q(t_0)) \geq V(q(t_0)) \quad (54)$$

where the inequalities provided in (49) and (52) were utilized.

Assume that $q(\tau) \in \mathbb{R}$ for $t_0 \leq \tau \leq t < \infty$ lies outside the ball $B(0, \Omega)$ as follows

$$\Omega < \|q(\tau)\|. \quad (55)$$

From (50) and (55), the following inequality can be determined

$$\dot{V}(q(\tau)) \leq -\gamma_3(\Omega) + \xi_0,$$

and hence, from the definition for Ω in (51), it is clear that

$$\dot{V}(q(\tau)) \leq 0. \quad (56)$$

By utilizing (54) and the result in (56), the following inequalities can be developed for some constant $\Delta\tau$

$$\gamma_1(d\Omega_1) \geq V(q(t_0)) \geq V(q(\tau)) \geq V(q(\tau + \Delta\tau)) \geq \gamma_1(q(\tau + \Delta\tau)). \quad (57)$$

Since $\gamma_1(\cdot)$ is a class \mathcal{K} function, (53) and (57) can be used to develop the following inequality

$$\|q(t)\| \leq d(\Omega_1) = (\gamma_1^{-1} \circ \gamma_2)(\Omega_1) + \gamma_1^{-1}(\xi_b) \quad \forall t \geq t_0 \quad (58)$$

provided the assumption in (55) is satisfied. If the assumption in (55) is not satisfied, then

$$\|q(t)\| \leq \Omega = \gamma_3^{-1}(\xi_0) \quad \forall t \geq t_0. \quad (59)$$

Hence, $q(t)$ is GUB for Case A.

The initial condition $q(t_0)$ lies inside the ball $B(0, \Omega)$ as follows

$$\|q(t_0)\| \leq \Omega \leq \Omega_1. \quad (60)$$

If $q(t)$ remains in the ball, then the inequality developed in (59) will be satisfied. If $q(t)$ leaves the ball, then the results from Case A can be applied. Hence, $q(t)$ is GUB for Case B. ■

³This proof is based on the proof for Theorem 2.14 in [32].